

ESTIMATION OF THE CENTRE OF ROTATION FOR A SHIP IN REAL SEA STATE ENVIRONMENT

Chen Zhang, University of Oldenburg, and Jade University of Applied Science, Germany

Alexander Härting, Jade University of Applied Science, Germany

Butteur Ntamba Ntamba, Cape Peninsula University of Technology, Cape Town, South Africa

Bernhard Schwarz-Röhr, Ghent University, Belgium, and Jade University of Applied Science, Germany

SUMMARY

Wave induced ship motions are composed of translations and rotations, but there is no unique pivot point. In this paper it is suggested to define a centre of rotation (CR) as the point where the linear accelerations experienced by a sensor are not affected by the rotations. Based on trials in a real sea state environment, a method is investigated to estimate the CR, which may not coincide with the centre of gravity. The angles are determined by high-pass filtering and integration of the measured angular rates. The linear accelerations are then transformed from the body-fixed frame to the horizontal inertial frame, the transformation including an initially unknown offset vector between the CR and the sensor, which is estimated by a Kalman filter. The results indicate that the CR position can indeed be determined uniquely. Its dependence on the relative motion of the vessel in the wave system carries useful information for wave spectrum analysis.

NOMENCLATURE

CR	Ship centre of rotation	R_{ψ}^T	Transformation matrix of yaw angle
s	State vector	ax_{off}	Acceleration caused by offset in x axis (m/s ²)
s_k	State vector at time k	ay_{off}	Acceleration caused by offset in y axis (m/s ²)
s_{k-1}	State vector at time k-1	az_{off}	Acceleration caused by offset in z axis (m/s ²)
F_k	State transition model	DP	Dynamic positioning
P_k	Error covariance matrix at time k		
Q_k	Covariance of process noise		
H_k	Observation model		
K_k	Kalman gain		
u	Observation vector		
u_k	Observation vector at time k		
R_k	Covariance of observation noise		
\hat{s}_k	Updated state vector at time k		
\hat{P}_k	Updated error covariance at time k		
I	Unitary matrix		
ax_n	Surge acceleration at CR (m/s ²)		
ay_n	Sway acceleration at CR (m/s ²)		
az_n	Heave acceleration at CR (m/s ²)		
r_x	Offset in x direction (m)		
r_y	Offset in y direction (m)		
r_z	Offset in z direction (m)		
ax_{sensor}	Surge acceleration from sensor (m/s ²)		
ay_{sensor}	Sway acceleration from sensor (m/s ²)		
az_{sensor}	Heave acceleration from sensor (m/s ²)		
ϕ	Roll angle (rad)		
θ	Pitch angle (rad)		
ψ	Yaw angle (rad)		
$\dot{\phi}$	Roll angular acceleration (rad/s ²)		
$\ddot{\theta}$	Pitch angular acceleration (rad/s ²)		
$\ddot{\psi}$	Yaw angular acceleration (rad/s ²)		
R_n^b	Transformation matrix from earth-fixed frame to ship body-fixed frame		
R_{ϕ}^T	Transformation matrix of roll angle		
R_{θ}^T	Transformation matrix of pitch angle		

1 INTRODUCTION

This work is part of a larger project that aims at determining the directional wave spectrum from ship motion measurements in deep and shallow water. Ship motions appear in translational (surge, sway and heave) and rotational (roll, pitch and yaw) degrees of freedom. The centre of rotation (CR) can be defined as the point where the linear accelerations are not affected by the rotations. The so defined CR cannot be expected to be rigidly fixed in the ship's body frame. However, its average can be determined and its displacement from the centre of gravity can be analysed in terms of parameters such as ship speed and wave incidence angle. It is expected that the position of the CR carries information on the sea state which can be exploited in the estimation of the directional wave spectrum.

In this paper a Kalman filter is presented that estimates the averaged CR position from motion measurements at an arbitrary point of the vessel. Sea trials on two vessels were performed to test the algorithm. Low cost sensors were used to measure linear accelerations and rotational rates. In the long term it is intended to use such a system routinely to provide motion data for the determination of the exciting sea state.

2 VESSELS & EXPERIMENTAL CONDITIONS

2.1 AGULHAS II

Agulhas II is a South African icebreaking Polar Supply and Research Vessel (PSRV), with its overall length of 134.2m, breadth of 22m, and under 7.65m draught. There were two sensor boxes with low-cost gyros and accelerometers installed on-board. One was placed on the observation deck above the navigation bridge recording both, linear accelerations and angular rates in three degrees-of-freedom at a rate of 8Hz. It was connected to a GPS receiver to provide accurate position and time. The other sensor was set up in the engine control room within a few metres of the ship's centre of mass. This sensor was producing all three linear accelerations but only roll and pitch angular rates at a frequency of 10Hz.

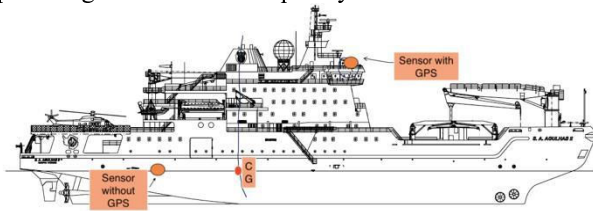


Figure 1. Agulhas II with sensor boxes on-board (Bekker and Omer, 2018, legends added by author)

The experiment was conducted on a voyage Cape Town-Antarctica- Cape Town from 28th June 2017 to 12th July 2017. To keep file sizes manageable, the sensors were operated for intervals of 2 to 5 hours at a time. Naturally, the recording intervals could not be identical for both sensors. After synchronising the sensor without GPS by using correlation, the angular rates showed a nearly perfect match. Then, the linear accelerations could be pre-processed with exactly corresponding time intervals. Finally, the estimation algorithm was applied independently to the motion of both sensors.

2.2 SIMON STEVIN

The Belgian vessel Simon Stevin was deployed for off-shore research and also as a training platform in the Southern North Sea and the eastern part of the English Channel. The overall length of Simon Stevin is 36m, with its breadth of 9.4m, and draught is 3.5m. There was a sensor box with low-cost gyros and accelerometers all in three dimensions on-board deployed, the recorded data was autonomously saved to a SD card, owned by Jade University of Applied Science.

The experiments were performed at 6-8 November 2017 in Belgian waters close to Ostend. The average water depth there was generally larger than 20m, but near a few sandbanks it was only 12m. The experiment consisted of a number of dedicated trial runs, each lasting for about 30 minutes at a specific speed with a constant heading, and then repeated at different parameter settings.

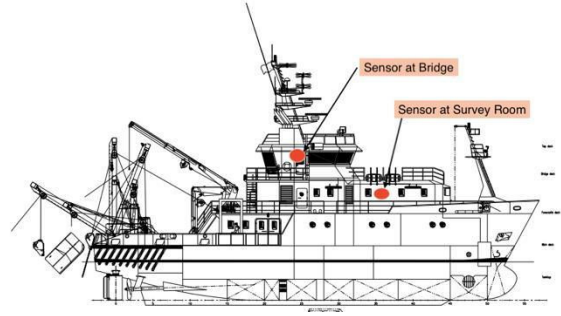


Figure 2. Simon Stevin with sensor boxes on-board (Damen shipyard, legends added by author)

3 MATHEMATIC MODEL

3.1 KALMAN FILTER

The Kalman filter is an algorithm which uses a series of measurements and produces the estimation of required variables under consideration of statistic uncertainties such that the result is more precise than based on a single measurement. The algorithm can be separated into a prediction and a correction part. In the prediction part, the required variables forming the state vector, here the linear accelerations at CR and the components of the offset vector $s=[ax_n, ay_n, az_n, r_x, r_y, r_z]$, are propagated in time from $k-1$ to k with the transition matrix F and the error covariance matrix P , as given in equations (1) and (2).

$$s_k = F_k s_{k-1} \quad (1)$$

$$P_k = F_k P_{k-1} F_k^T + Q_k \quad (2)$$

In the correction part, the predicted state vector s_k is adjusted based on the difference between the actual measurements, here $u=[ax_{\text{sensor}}, ay_{\text{sensor}}, az_{\text{sensor}}]$, and the expected observations $H_k s_k$. For that purpose, the Kalman gain matrix K is computed, which is then also used to update the error covariance matrix P . The required calculation steps are shown in equations (3) to (5).

$$K_k = P_k H_k^T (R_k + H_k P_k H_k^T)^{-1} \quad (3)$$

$$\hat{s}_k = s_k + K_k (u_k - H_k s_k) \quad (4)$$

$$\hat{P}_k = (I - K_k H_k) P_k (I - K_k H_k)^T + K_k R_k K_k^T \quad (5)$$

3.2 EULER TRANSFORMATION

From the sensor boxes on-board, three dimensional linear accelerations are acquired in the ship body-fixed frame. Nevertheless, the ship linear motions at CR are needed in the earth-fixed inertial frame. By integrating and high-pass filtering the measured angular rates, the angles could be determined independently. Then the three Euler angles roll, pitch and yaw can be utilized to transform from the earth-fixed frame to the ship body-fixed frame by applying the transformation matrix R_n^b , as described in equation (6). The individual rotation matrices R_ϕ^T , R_θ^T , R_ψ^T are formed from the Euler angles as shown in equations (7) to (9).

$$R_n^b = R_\phi^T \cdot R_\theta^T \cdot R_\psi^T \quad (6)$$

$$R_\phi^T = \begin{pmatrix} 1 & 0 & 0 \\ 0 & \cos\phi & \sin\phi \\ 0 & -\sin\phi & \cos\phi \end{pmatrix} \quad (7)$$

$$R_\theta^T = \begin{pmatrix} \cos\theta & 0 & -\sin\theta \\ 0 & 1 & 0 \\ \sin\theta & 0 & \cos\theta \end{pmatrix} \quad (8)$$

$$R_\psi^T = \begin{pmatrix} \cos\psi & \sin\psi & 0 \\ -\sin\psi & \cos\psi & 0 \\ 0 & 0 & 1 \end{pmatrix} \quad (9)$$

$$\begin{pmatrix} ax_{sensor} \\ ay_{sensor} \\ az_{sensor} \end{pmatrix} = \left(R_n^b \cdot \begin{pmatrix} ax_n \\ ay_n \\ az_n + g \end{pmatrix} + \begin{pmatrix} ax_{off} \\ ay_{off} \\ az_{off} \end{pmatrix} \right) =$$

$$\begin{pmatrix} ax_n \cos\theta \cos\psi + ay_n \cos\theta \sin\psi - az_n \sin\theta - g \sin\theta + r_z \ddot{\theta} \\ ax_n (\sin\phi \sin\theta \cos\psi - \cos\phi \sin\psi) + ay_n (\sin\phi \sin\theta \sin\psi + \cos\phi \cos\psi) + az_n \sin\phi \cos\theta + g \sin\phi \cos\theta - r_z \ddot{\phi} \\ ax_n (\cos\phi \sin\theta \cos\psi + \sin\phi \sin\psi) + ay_n (\cos\phi \sin\theta \sin\psi - \sin\phi \cos\psi) + az_n \cos\phi \cos\theta + g \cos\phi \cos\theta + r_y \ddot{\phi} - r_x \ddot{\theta} \end{pmatrix} \quad (11)$$

4 RESULTS

4.1 RESULTS OF AGULHAS II

In the following, the origin of the ship coordinate system is placed in the centre of gravity as given by the loading computer. According to the right-hand rule, the three axes are pointing to bow, port and upward. For a rigid body the estimated CR position should not depend on the position of the sensor. For testing two sensors at different positions were used on the Agulhas II. Sensor I was placed in the engine control room without GPS, somewhat behind the

The accelerations at the offset point produced by the rotations can be expressed by equation (10).

$$\begin{pmatrix} ax_{off} \\ ay_{off} \\ az_{off} \end{pmatrix} = \begin{pmatrix} \ddot{\phi} \\ \ddot{\theta} \\ \ddot{\psi} \end{pmatrix} \times \begin{pmatrix} r_x \\ r_y \\ r_z \end{pmatrix} = \begin{pmatrix} \ddot{\theta} r_z - \ddot{\psi} r_y \\ \ddot{\psi} r_x - \ddot{\phi} r_z \\ \ddot{\phi} r_y - \ddot{\theta} r_x \end{pmatrix} \quad (10)$$

Thus after combining equations (6) to (10), the total acceleration at the sensor is given by equation (11).

centre of gravity. Its coordinates in the ship frame were estimated as (-8m, 0, 0), the x-position being rather uncertain. Sensor II was on the observation deck with GPS calibration, and its position in the ship frame could fairly accurately be measured to be (12.7m, 0m, 22.3m). For analysis, data sets were selected, where the ship was at a constant heading for several hours and the exciting wave system was dominated by a long-crested swell. The results for the estimated CR positions are shown in Table 1. As the CR may depend on the environmental conditions, the positions may be different for each data set. However, both sensors should yield consistent results.

Table 1. Results of selected Agulhas II sea trials

Data Set	Relative Angle [°]	Ship Speed [kn]	CR by Sensor I			CR by Sensor II		
			[m]			[m]		
			x	y	z	x	y	z
25&118	130 Port	0 (DP)	-6.7	-8.3	12.4	-10.7	-9.8	20.7
28&121	135 Port	7.5	-13.8	-13.1	2.5	-15.6	-10.6	9.9
38&135	130 Port	9.9	-15.4	-5.3	2.6	-16.4	-3.7	9.8
57&160	30 Port	13.5	-15	-13.9	-3.3	-13.2	-10.9	10.3
59&162	20 Port	13	-14.2	-13.4	-1.4	-11.7	-10.6	12.5

To assist analysis and interpretation of the results, Figure 3-10 have been prepared. Data set 25&118 has been omitted because the ship was in dynamic positioning mode and the thruster activity may have altered the dynamic behaviour. For each of the other data sets there are two figures. The first shows a small section of the time series for the linear accelerations, the other shows the estimated sensor offset from the CR for the full measurement period of several hours.

As for the linear accelerations, the labels I sensor and II sensor represent the measurements directly at the sensor boxes, while labels I filtered and II filtered are defined to be the linear accelerations estimated by the Kalman filter. These are supposed to be the linear accelerations at the ships's CR and, therefore, these two lines should be identical.

As can be seen from Figure 3, 5, 7 and 9, the agreement varies from fair to nearly perfect. In heave the match is always good, while in surge and sway some discrepancies

appear in Figure 7 and 9. Note, however, that in the latter cases the absolute amplitude is small, the ship travels at high speed almost into the waves, while, in Figure 3 and 5, wave incidence is more broadside.

Looking at the estimated CR-offsets from the sensors (Figure 4, 6, 8 and 10) it can be said that the Kalman filter arrives at more or less stable, but not really constant values. Variations appear with a time characteristic of several minutes and a standard deviation of typically 2 m. It should be pointed out that the shape of the curves agrees very closely between the two sensors. The average values, after the Kalman filter has reached a settled state, are then subtracted from the sensor positions to give the CR-positions listed in table 1. The analysis indicates that, internally, the filter results are unique, which is corroborated by studying the covariance. Yet, the difference between the results achieved by the two sensors cannot be completely explained by the remaining statistic uncertainty.

The CR as defined in this paper is not a rigidly fixed point in the ship. There will be rapid variations within a wave period or an eigen period of the ship motion. In a wave slope reaching the ship inclined to starboard or port, the instantaneous CR will not be the same. For the average CR a characteristic dependence on the ship speed and the wave incidence angle can be expected.

Looking at the data sets in Table 1 as can be seen that, with waves coming from port, the CR is always displaced to starboard from the midship plane, which would intuitively seem plausible. Unfortunately, there were no suitable data sets available with waves coming from starboard.

Comparing the columns in Table 1, the x- and y-coordinates of the estimated CR-position agree rather well between the two sensors. However, there is a systematic discrepancy in the z-coordinate. The values reached by sensor II seem to be too high by a considerable amount.

A preliminary analysis indicates that the reason may lie in small errors in the angles entering the transformation (chapter 3.2). The comparatively large gravitational acceleration g could easily corrupt the lateral accelerations, on which the estimated z-coordinate critically depends. Sensor I, being closer to the CR, is affected much less. More detailed investigations into this problem are under way.

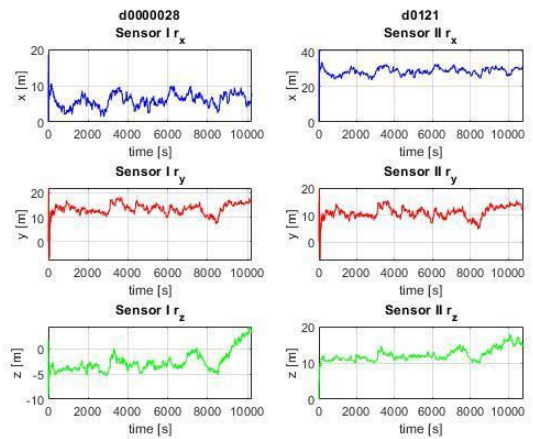


Figure 4. Offset estimation of 28&121

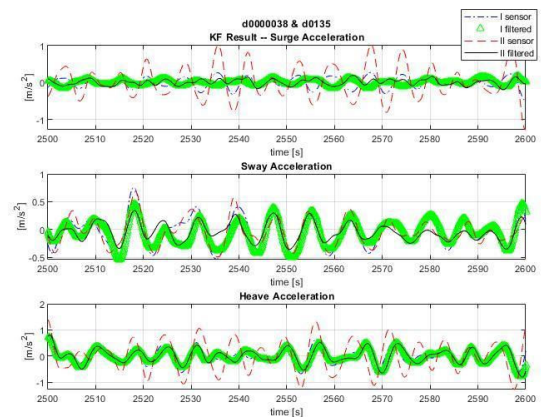


Figure 5. Linear motion of 38&135

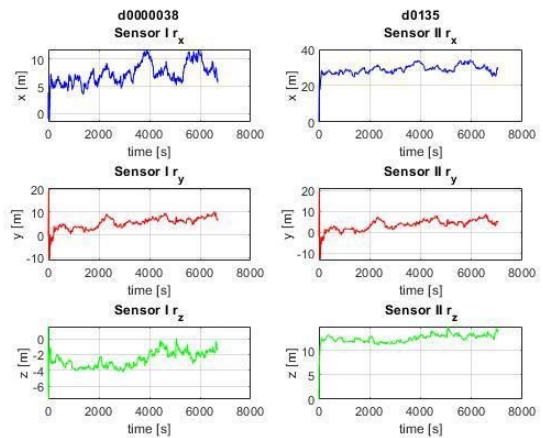


Figure 6. Offset estimation of 38&135

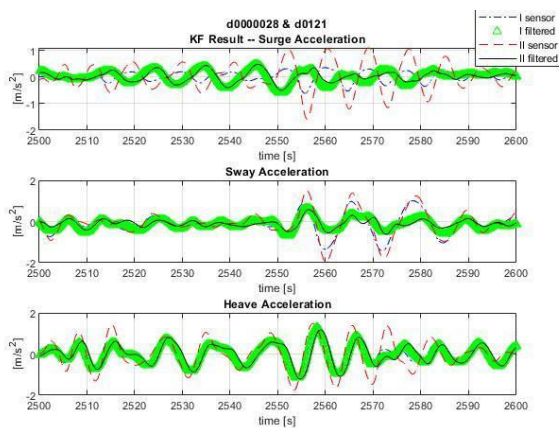


Figure 3. Linear motion of 28&121

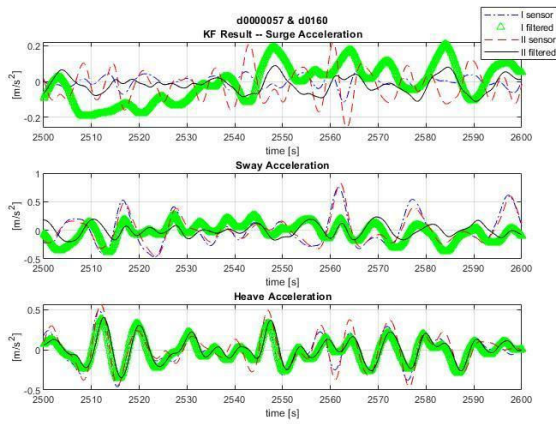


Figure 7. Linear motion of 57&160

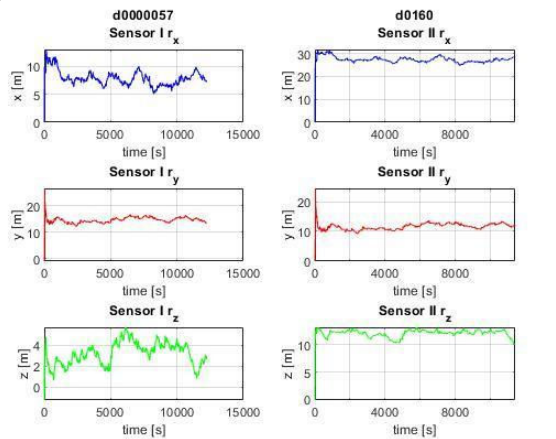


Figure 8. Offset estimation of 57&160

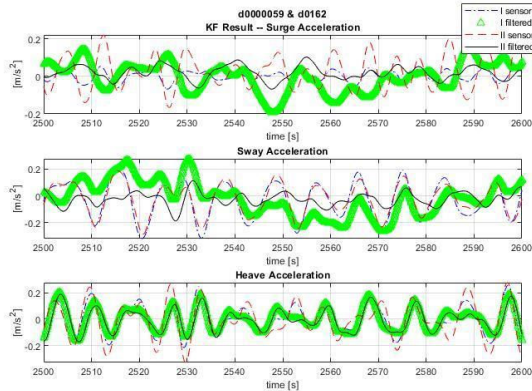


Figure 9. Linear motion of 59&162

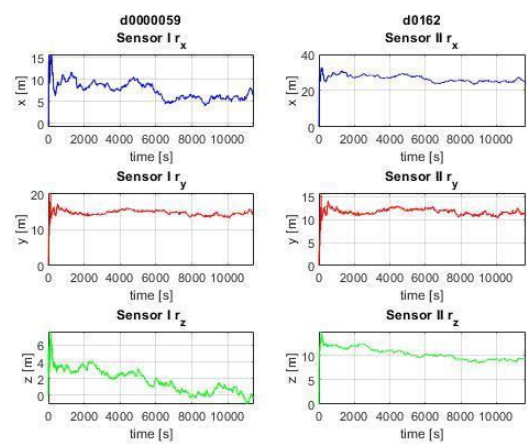


Figure 10. Offset estimation of 59&162

4.2 RESULTS OF SIMON STEVIN

There were two sensor boxes installed on Simon Stevin, as shown in the arrangement plan (chapter 2.2). As with the Agulhas II, the origin of the ship coordinate system is placed in the centre of gravity and the three axes are pointing to bow, port and upward. Up to now, only data from the sensor on the bridge have been analysed. Its position in the ship frame was determined to be (0.21m, 3.15m, 8.29m).

In Figure 11 and 12, the estimation of the offset vectors is presented for two data sets. The settling time until the filter reaches constant values is similar to the Agulhas samples, noting the much shorter duration of an individual trial run. After the adjusting period small oscillations can be observed with standard deviations of typically 0.1m, in fair agreement with the filter covariance. The results indicate that the offset vector between the sensor and the CR has been found uniquely for all of the investigated data sets.

The estimated CR positions for Simon Stevin are displayed in Table 2. The data set numbers, representing the sequence of sea trials, have been arranged by wave incidence angles. The numbers in last column of Table 2 are obtained by averaging the offsets after settling and then transforming them to the ship coordinated system. The estimated CR position appears to be quite stable when comparing data sets taken under similar external conditions, as for example data sets 21 and 23. In Table 2, the x-components of the CR position are always in front of the CG with rather constant values, except for the last two rows.

Looking at data sets 10 and 14 as another example, there are practically symmetric conditions between port and starboard. As expected, the y-component of the CR position changes sign, but the absolute values are significantly different. Also from the other data sets a general tendency to port can be identified. Investigating the z-component, data sets 4, 13 and 9, 18 are examples with port/starboard symmetry. In data sets 9, 18 the resulting value is lower, but there, also, the ship speed is much slower than in data sets 4, 13. Throughout the data

sets the z-component is in a reasonable range, except for data sets 2 and 3.

Variations in the estimated CR positions are certainly produced by different ship speed and wave conditions. However, not all of the variations in Table 2 can be explained by simple arguments. It must be noted that, in Table 2, wave characterization was reduced to the peak incidence angle. The actual wave spectra encountered in the area of the experiment was much more complex with a wide spread in angles and frequencies. Rudder action by the autopilot may have had an influence, especially on a small ship like the Simon Stevin. Finally, residual errors in the angle transformation may have led to errors in the estimation of the z-component of the CR position. At least some of these questions may be answered by the ongoing analysis of data from the second sensor in the survey room.

The results so far indicate that the CR position varies according to external factors, such as wave length, period and direction and the ship's seakeeping behaviour. Nevertheless, for an individual trial run with nearly constant conditions, a unique CR location can be produced.

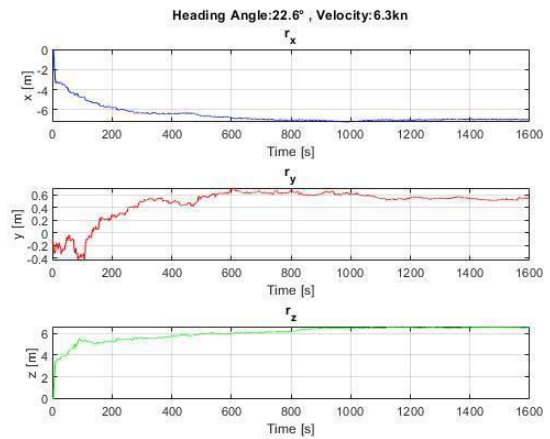


Figure 11. Offset estimation of data 21

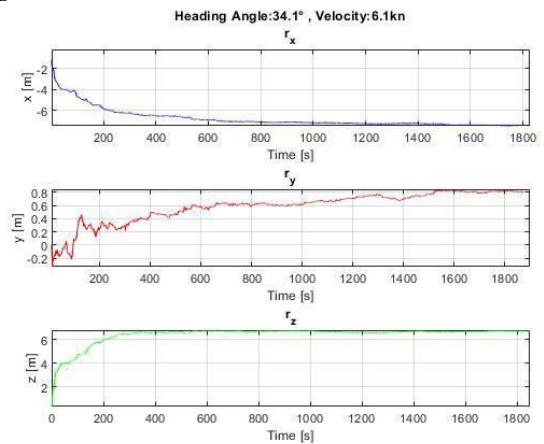


Figure 12. Offset estimation of data 23

Table 2. Results of selected Simon Stevin sea trials

Data Set	Relative Angle		Ship Speed [kn]	CR in ship frame [m]		
	[°]			x	y	z
1	142	Port	6.1	7.04	2.69	2.05
12	130	Port	4.2	7.46	2.55	1.73
4	167	Port	6.1	7.91	2.16	0.51
13	165	Port	9.5	8.03	2.77	0.88
15	176	Port	3.7	8.23	1.98	1.31
21	152	Port	6.3	7.39	2.63	1.7
23	155	Port	6.1	7.4	2.41	1.66
3	44	Port	5.8	9.44	4.37	-2.3
10	48	Port	3.8	7.03	3.78	1.18
9	167	Starboard	3.8	10.36	0.59	-0.5
18	165	Starboard	3.8	9.86	0.31	-1.05
2	45	Starboard	6.7	14.9	-1.45	-2.62
14	51	Starboard	3.8	11.26	-0.47	-1.64

5 CONCLUSIONS

The Kalman filter algorithm, coping with the influence of geometrical offsets and with the assistance of Euler transformation can be utilized to determine the ship's CR position. From data of all investigated sea trials, it is safe to conclude that the algorithm as such is proven. The results appear to be quite sensitive to variations of ship velocity and incident wave characteristics. It is therefore worthwhile to develop a mathematical model for the dependence of the CR position on the various influence parameters. Then, for estimating the directional wave spectrum from ship motions, the CR position can provide additional information, e.g. for port-starboard ambiguity resolution.

6 ACKNOWLEDGEMENTS

The authors are grateful to the crews of Agulhas II and Simon Stevin for their great help and pleasant cooperation.

7 REFERENCES

Abankwa, Nana O., et al, 2015. Ship motion measurement using an inertial measurement unit, in: the 2nd World Forum on Internet of Things. Milan, Italy. <https://ieeexplore.ieee.org/document/7389083>

Bekker, A., Omer, H., 2018. Human responses to wave slamming vibration on a polar supply and research vessel. *Applied Ergonomics* 67. 71-82. <https://doi.org/10.1016/j.apergo.2017.09.008>

Fossen Thor I., 2011, Kinematics, in: Handbook of Marine Craft Hydrodynamics and Motion Control. pp. 15–33. <https://onlinelibrary.wiley.com/doi/book/10.1002/9781119994138>.

Kalman, R., E., 1960. A new approach to linear filtering and prediction problems. *Journal of Basic Engineering*. 35-45. <http://fluidsengineering.asmedigitalcollection.asme.org/article.aspx?articleid=1430402>.

Soal, K., Bienert, J., Bekker, A., 2015. Operational modal analysis on the polar supply and research vessel the S.A. Agulhas II, in: the 6th International Operational Modal Analysis Conference. Gijon, Spain. https://www.researchgate.net/publication/280445237_Operational_Modal_Analysis_on_the_Polar_Supply_and_Research_Vessel_the_SA_Agulhas_II.

Linder J., Enqvist, M., Fossen, T. I., Johansen, T. A., Gustafsson, F., 2015. Online estimation of ship's mass and centre of mass using inertial measurements, in: the 10th IFAC Conference on Manoeuvring and Control of Marine Craft. Copenhagen, Denmark. pp. 134-139.

<https://www.sciencedirect.com/science/article/pii/S2405896315021618>.

Pascoal, R., Guedes Soares, C., 2009. Kalman filtering of vessel motions for ocean wave directional spectrum estimation. *Journal of Ocean Engineering*. 477-488. <https://www.sciencedirect.com/science/article/pii/S0029801809000183>

Product Sheet of Fishery Research Vessel 3609 Simon Stevin, <https://products.damen.com/en/ranges/fishery-research-vessel/frv-3609>.

Triantafyllou, M. S., Bodson, M., Athans, M., 1983. Real Time estimation of ship motions using Kalman filtering techniques. *IEEE Journal of Oceanic Engineering*. 9-20. <https://ieeexplore.ieee.org/document/1145542>

8 AUTHORS BIOGRAPHY

Chen Zhang received her bachelor and master degree from Northwestern Polytechnical University, China in 2010 and 2013 respectively. Now she is a PhD candidate in the Department of Computer Science, Carl von Ossietzky University of Oldenburg, Germany. Her research interests contain measurement and analysis of ship movements at sea states, also including motion control.

Alexander Härting is a professor in Department of Maritime Studies, Jade University of Applied Science, Germany. His research interests include measurement and analysis of dynamic ship movements in seaway, integration of different navigation sensors, and measurement of the squat of seagoing vessels in narrow fairways.

Butteur Ntamba Ntamba hold a bachelor degree in mechanical engineering from University of Lubumbashi, Democratic Republic of Congo and a master degree from Cape Peninsula University of Technology (CPUT), South Africa. He is now a lecturer in the Faculty of Engineering and a PhD candidate with CPUT. His research work is on ship response in waves.

Bernhard Schwarz-Röhr holds his diploma degree of physics, and now he is a PhD candidate in Faculty of Engineering and Architecture, Ghent University, Belgium. He is responsible for wave estimation, sea state analysis, and measurement of ship movements.